Poly(lactic acid) Properties as a Consequence of Poly(butylene adipate-*co*-terephthalate) Blending and Acetyl Tributyl Citrate Plasticization

Maria-Beatrice Coltelli,[1] Irene Della Maggiore,[2] Monica Bertoldo,[3] Francesca Signori,[2] Simona Bronco,[3] Francesco Ciardelli[2,3]

[1]*Centro Italiano Packaging and Dipartimento di Chimica e Chimica Industriale, via Risorgimento 35, 56126 Pisa, Italy*
[2]*Dipartimento di Chimica e Chimica Industriale dell'Università di Pisa, via Risorgimento 35, 56126 Pisa, Italy*
[3]*Laboratorio Regionale per le Applicazioni Industriali dei Polimeri-Consiglio Nazionale delle Ricerche-Istituto Nazionale per la Fisica della Materia (PolyLab-CNR-INFM) c/o Dipartimento di Chimica e Chimica Industriale, via Risorgimento 35, 56126 Pisa, Italy*

Received 21 December 2007; accepted 30 March 2008
DOI 10.1002/app.28512
Published online 14 July 2008 in Wiley InterScience (www.interscience.wiley.com).

ABSTRACT: This study was aimed at the modulation of poly(lactic acid) (PLA) properties by the addition of both a low-molecular-weight plasticizer, acetyl tributyl citrate (ATBC), and a biodegradable aliphatic–aromatic copolyester, poly(butylene adipate-*co*-terephthalate) (PBAT). PLA/PBAT, PLA/ATBC, and PLA/PBAT/ATBC mixtures with 10–35 wt % ATBC and/or PBAT were prepared in a discontinuous laboratory mixer, compression-molded, and characterized by thermal, morphological, and mechanical tests to evaluate the effect of the concentration of either the plasticizer or copolyester on the final material flexibility. Materials with modulable properties, Young's modulus in the range 100–3000 MPa and elongation at break in the range 10–300%, were obtained. Moreover, thermal analysis showed a preferential solubilization of ATBC in the PBAT phase. Gas permeability tests were also performed to assess possible use in food packaging applications. The results are discussed with particular emphasis toward the effects of plasticization on physical blending in the determination of the phase morphology and final properties. © 2008 Wiley Periodicals, Inc. J Appl Polym Sci 110: 1250–1262, 2008

Key words: additives; blending; glass transition; polyesters

INTRODUCTION

Poly(lactic acid) (PLA) has received attention for large-scale industrial applications, as the building of big synthesis plants[1] has allowed effective price reduction. The advantage over traditional materials is mainly environmental, as PLA is obtained from renewable resources,[2] and it is compostable as well, which allows for easier waste management with respect to traditional synthetic plastics.[3] PLA-based materials could be successfully used in packaging applications, as they have properties that allow the replacement of conventional hydrocarbon-based packaging.[4,5] PLA can be processed in the 150–200°C temperature range by injection molding, sheet extrusion, blow molding, thermoforming, and film forming, but the obtained material is usually stiff and brittle. Therefore, a modulation of its mechanical properties is needed for this material to be used in applications actually reserved to polyolefins. For this purpose, both the addition of plasticizers and blending with other biodegradable polymers were recently explored.

Plasticizers can be added to PLA to decrease its glass-transition temperature (T_g), which results in a lower stress at yield and a higher elongation at break[6,7] at room temperature, with these conditions being necessary to improve the flexibility of films and sheets. With this concern, either glycerol[8,9] and its ester derivatives, such as diglycerine tetraacetate, glyceryl triacetate,[10] and acetyl glycerol monolaurate,[11] have been added to PLA. The former was not very efficient in reducing T_g, whereas the last two allowed 60 and 100 times increases in the elongation at break with respect to pure PLA, respectively. Citrate derivatives, such as tributyl citrate,[8] acetyl triethyl citrate,[12] and acetyl tributyl citrate (ATBC), have also been added to PLA and provided similar results. Labrecque et al.[13] compared the plasticizing efficiency of triethyl and tributyl citrates and their acetyl derivatives and found out a very similar trend in the thermomechanical properties, with ATBC providing the lowest glass-transition value. Moreover, triethyl citrate migrated preferentially from PLA in a

Correspondence to: M.-B. Coltelli (beacolt@ns.dcci.unipi.it).

Contract grant sponsor: Ministero dell'Università e della Ricerca - Fondo pergli Investimenti della Ricerca di Base (MIUR-FIRB) 2003 D. D. 2186; contract grant number: RBNE03R78E.

TABLE I
Technical Data of the Polyesters Used in this Study

	Density (g/cm^3)[a]	M_n ($\times 10^{-4}$)[b]	M_w ($\times 10^{-4}$)[b]	I_d[b,c]	MFR (g/10 min)
P1	1.25	8.41	17.8	2.1	6.4 ± 0.8
P2	1.24	12.0	21.1	1.7	4.7 ± 0.7
PBAT	1.26	3.67	9.54	2.6	24 ± 4

M_n = number-average molecular weight; M_w = weight-average molecular weight.
[a] From technical data sheets.
[b] From gel permeation chromatography analysis ($CHCl_3$, 1 mL/min, polystyrene standards, PLgel-Mixed-D).
[c] $I_d = M_w/M_n$.

wet state, as it is soluble in water.[14] Similar results were obtained by Baiardo et al.[15] for solution-cast and melt-extruded blend films. Moreover, by using different plasticizers, they correlated the mechanical properties, such as strain at break, tensile strength, and elastic modulus, to the PLA T_g, showing the change from brittle to ductile behavior when the T_g value was about 35°C. To balance the opposite necessities of decreasing the material glass transition and limiting the migration of plasticizers, Ljungberg and Wesslen[16,17] synthesized oligomers of tributyl citrate with different molecular weights. The tertiary hydroxyl group of tributyl citrate seemed to have participated to the oligomerization and caused uncontrolled branching. The trimer or eptamer addition to PLA resulted in phase separation at 20 and 15 wt % concentrations, respectively, with saturation concentration decreasing with increasing plasticizer molecular weight.

Poly(ethylene glycol) (PEG)[13,18,19] at different molecular weights has shown similar behavior to citrate derivatives. The main difference was the PEG crystal attitude to nucleate cold PLA crystallization. No difference was observed when monomethyl ether of PEG was used on either T_g or the ability of PLA to crystallize.[20] Similarly to PEG, poly(propylene glycol) (PPG)[21,22] plasticized PLA but did not promote crystallization. PPG creates tiny pools of liquids, which may locally plasticize PLA during deformation and positively affect the drawability.

The plasticizing effect of oligomeric malonate esteramides and polyesters[23] induced a decrease of 11–17°C in the glass transition, and the oligomeric copolyamide containing the less hindered amine was the most effective. The authors ascribed this result to the possibility of hydrogen bond formation.

The glass transition value of PLA is also slightly affected by humidity, and in particular, it follows the Gordon–Taylor relationship as a function of water content.[24]

Blends of PLA with other biodegradable polyesters have also been widely investigated to prepare soft or more flexible materials for many different applications. To easily achieve property modulation, the crucial point seems to be the miscibility and compatibility between the phases. In fact, all of the investigated biodegradable polyesters, including poly(hydroxyl butyrate),[25] poly(butylene succinate),[26] polycaprolactone,[27,28] and poly(butylene adipate-*co*-terephthalate) (PBAT),[29,30] are immiscible with PLA. The latter allowed the preparation of materials with interesting mechanical properties, such as a good level of toughness.[31] As the final properties of blends depend on the composition, level of compatibility, processing, and morphological features, only a rough modulation of properties was possible through the blending approach.

For these reasons, the development of plasticized multiphase systems, such as plasticized PLA blends[32] and nanocomposites,[9,19,33] have recently been investigated with the aim of finely tuning mechanical properties, but the reciprocal effects of the plasticization and toughening were not taken properly into account. In particular, the effect of plasticization on the properties of toughened blends with similar properties but based on PLAs of different grades and the possible overall preferential distribution of plasticizer into one polymer phase have never been considered.

In this framework, the fine modulation of PLA properties was investigated by the addition of both a low-molecular-weight plasticizer (ATBC) and a biodegradable polyester (PBAT). The blends of different compositions were prepared in a discontinuous laboratory mixer, compression-molded, and finally characterized by thermal, morphological, mechanical, and permeability tests. The attention was focused, in particular, on the concentration effects of the plasticizer and copolyester on the final properties, particularly on the enlightenment of the effects of preferential solubilization of the plasticizer and the reciprocal influence of plasticization and toughening.

EXPERIMENTAL

Materials

Two different PLAs, 2002D film-grade PLA (P1) and 4042D extrusion/thermoforming-grade PLA (P2),

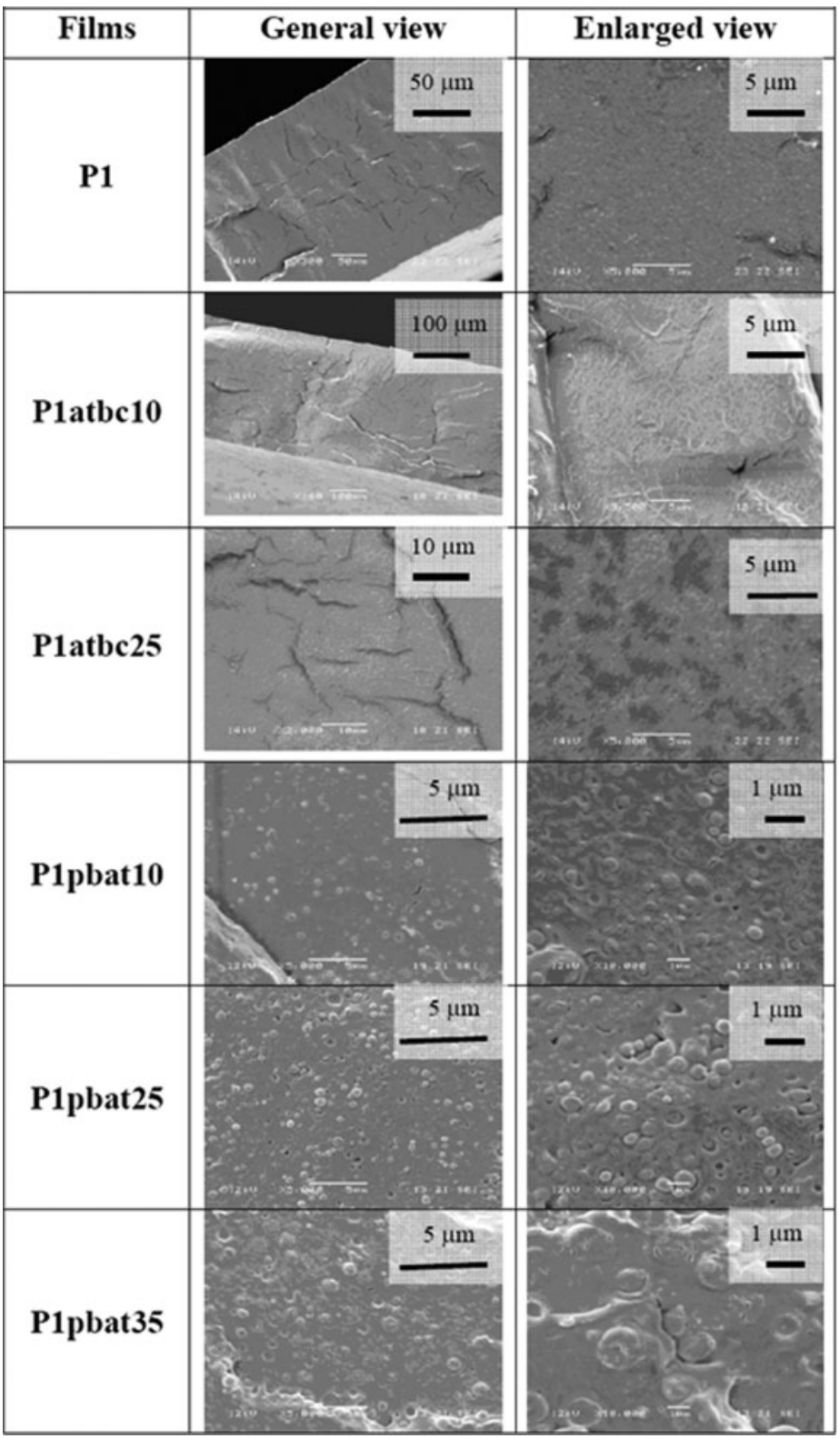

Figure 1 SEM micrographs of the cryogenically broken surfaces of the films made of P1, P1 with 10% ATBC (P1atbc10) and 25% ATBC (P1atbc25), and P1 with 10% PBAT (P1pbat10), 25% PBAT (P1pbat25), and 35% PBAT (P1pbat35).

purchased from Cargill Dow (Bair, US-NE), were used in this study. PBAT, Ecoflex FBX7011, was purchased from BASF. The main characteristics of the polymers are reported in Table I. ATBC was purchased from Sigma-Aldrich (Milano, Italy) and was used as received.

TABLE II
Thermal Properties of the P1, P1/ATBC, and P1/PBAT Mixtures

Sample	Additive over PLA	T_g (°C)	ΔH_{cc} (J/g)[a]	T_{cc} (°C)	ΔH_m (J/g)[b]	T_m (°C)	ΔH_{mc} (J/g)[b]	Percentage crystallinity of PLA after quenching[a,c]
P1	0	60.1	—	—	0	—	—	~ 0
PBAT	0	−33.3	−15.29	−1.63	18.2	108	—	—
ATBC	0	−82.4	—	—	—	—	—	—
P1atbc10	10 wt % ATBC	44.1	−17.5	112	26.3	145	8.8	10.3
P1atbc25	25 wt % ATBC	30.3	−19.1	94	22.4	146	3.4	4.5
P1atbc35	35 wt % ATBC	27.4	−24.8	108	26.4	144	1.6	2.3
P1pbat10	10 wt % PBAT	60.2	−12.2	127	12.7[b]	152	0.6[b]	0.7[c]
P1pbat25	25 wt % PBAT	60.0	−2.8	131	3.9[b]	152	1.1[b]	1.5[c]
P1pbat35	35 wt % PBAT	61.1	−2.9	133	3.0[b]	152	0.3[b]	0.4[c]

[a] The enthalpies and crystallinity were calculated on the actual PLA content.
[b] In the calculation, ΔH_m of PBAT was neglected.
[c] For the calculation of crystallinity content, the enthalpy of totally crystalline PLA was assumed to be $\Delta H_0 = 93$ J/g.[17]

Preparation of the blends and compounds

PLA/PBAT blends and PLA/ATBC compounds were prepared in a discontinuous Brabender laboratory mixer (Duisburg, Germany) with a mixing chamber of 30 mL at 200°C with a blade rate of 50 rpm and a blending time of 10 min. Binary PLA/PBAT and PLA/ATBC mixtures were named P*x*pbat*y* or P*x*atbc*y*, where *x* indicates the PLA grade (P1 or P2) and *y* is the percentage by weight of PBAT or ATBC with respect to 100 g of PLA.

The preparation of the PLA/PBAT/ATBC blends was carried out in a discontinuous Brabender laboratory mixer with a mixing chamber of 50 mL at 200°C with a blade rate of 50 rpm and a blending time of 10 min. The ternary blends were named P*x*p*y*atbc*z*, where *x* indicates the PLA grade (P1 or P2), *y* is the percentage of PBAT in 100 g of the polymer blend, and *z* is the percentage by weight of ATBC calculated with respect to PLA (e.g., 10.9 g of P1p10atbc10 was composed of 9 g of PLA, 1 g of PBAT, and 0.9 g of ATBC).

The torque trend was recorded by the mixer equipment as a function of time. The material recovered from the mixer was compression-molded with a PM 20/20 Campana instrument (Milano, Italy) at 5 MPa and 200°C (for 2 min).

Characterization

Differential scanning calorimetry (DSC) measurements were performed with a Mettler Toledo DSC 822e (Milano, Italy) with STARe software version 6.10. Standard aluminum pans with 10–20 mg of sample were used. For P1-based compounds and blends, a first heating scan program from 30 to 220°C at 10°C/min was followed by a cooling step at −10°C/min up to −80°C and a successive heating step at 10°C/min up to 220°C. For P2-based blends, a first heating scan program from 25 up to 250°C at 20°C/min was followed by a quenching step in liquid nitrogen and by a second heating up to 250°C at 10°C/min under a nitrogen atmosphere. Thermogravimetric analyses were carried out in the Mettler Toledo STARe system with a thermogravimetric analyzer/standardized differential thermal analysis (SDTA) module in the range 25–600°C at a rate of 10°C/min under a 60-mL/min nitrogen flow.

The melt flow rate (MFR), expressed in grams of material per 10 min, was determined with a CEAST

TABLE III
Tensile Properties of the P1, PBAT, P1/ATBC, and P1/PBAT Mixtures

Sample	Modulus (MPa)	Stress at yield (MPa)	Strain at yield (%)	Stress at yield (%, MPa)	Strain at break (%)
P1	2996 ± 52	33 ± 7	2.4 ± 0.9	26 ± 4	13 ± 3
PBAT	66 ± 12	5 ± 2	15 ± 6	15 ± 7	670 ± 84
P1atbc10	2340 ± 89	29 ± 9	1.5 ± 0.9	19 ± 5	85 ± 14
P1atbc25	230 ± 70	13 ± 8	133.8 ± 37	22 ± 6	254 ± 26
P1atbc35	1500 ± 1000	20 ± 12	37 ± 25	22 ± 9	132 ± 66
P1pbat10	2882 ± 124	36 ± 8	1.5 ± 0.6	12 ± 5	17 ± 8
P1pbat25	2425 ± 136	30 ± 12	1.4 ± 0.8	24 ± 8	97 ± 23
P1pbat35	2182 ± 241	27 ± 9	1.5 ± 0.7	23 ± 9	91 ± 31

The specimens were obtained from compression-molded films.

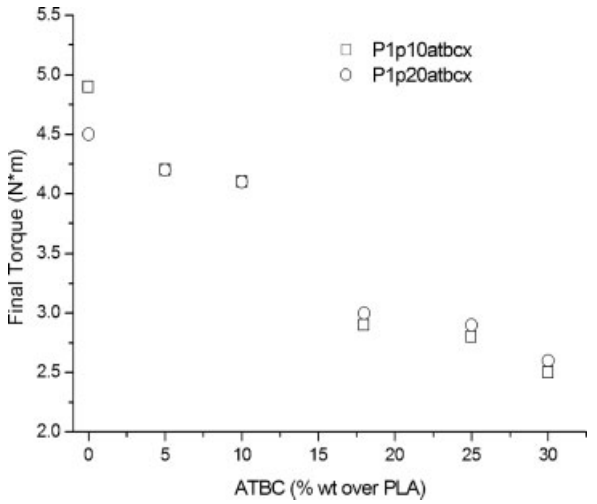

Figure 2 Final torque as a function of ATBC content in the ternary PLA/PBAT/ATBC mixtures.

module PIN 7026 melt flow instrument (Torino, Italy) equipped with VisualMELT software, which provided the melt volume rate data. The MFR was measured at 190°C with a weight of 2.16 kg (ASTM D 1238), following an ISO1133A standard procedure. The samples were kept for 2 h in a 60°C preheated vacuum oven before the MFR test to remove humidity.

The tensile properties were tested at room temperature (27°C) with a 500-N load cell and a crosshead speed of 1 mm/min with a Tinius Olsen tensile tester (Saldfords, UK). The specimens (ASTM D 628, type MIII) were cut from compression-molded films with a thickness of about 200 μm that were conditioned at least for 2 days at 50% relative humidity (RH) before testing. Each reported value is an average of measurements carried out on at least six specimens.

The O_2 permeability was measured with an ExtraSolution Permeo$_2$ instrument (Pisa, Italy) at 23°C and 0% RH on 50-cm^2 films according to the ASTM D 3985-02 norm. The permeability to CO_2 was measured with an ExtraSolution Permeo$_2$ instrument at 23°C and 0% RH on 50-cm^2 films according to the DIN 53380 norm, whereas the permeability to water vapor was measured with an ExtraSolution Permeo$_2$ instrument at 23°C and 85% RH on 50-cm^2 films according to the DIN 53122 norm.

The dipole momentums of the ATBC, PLA fragment, and PBAT fragment were calculated with CS CHEM3D ULTRA 7.0 software (Cambridge, MA), by achievement of the minimum energy configuration through a molecular orbital package (MOPAC), in the AM1 closed-shell computational method.

Scanning electron microscopy (SEM) characterization was carried out with a Jeol JSM model T-300 instrument on cryofractured and gold-sputtered samples. The determination of the diameter should have required the etching of PBAT from the cryogenically smoothed surface of the samples, but this procedure was not possible because a selective solvent could not be identified, although solubilization tests were performed with chloroform, methanol, ethanol, 1,1,1,3,3,3-hexafluoro-2-propanol, tetrahydrofuran, acetone, ethyl acetate, toluene, trichlorobenzene, benzyl alcohol, xylene, decaline, and *n*-hexane. Hence, we carried out the analysis on nonetched cryogenically fractured surfaces by taking into account the values obtained for at least 100 dispersed PBAT domains with Image Tool 3.0 software (San Antonio, TX).

RESULTS

PLA/ATBC and PLA/PBAT binary mixtures

Binary PLA mixtures were prepared by the mixture of P1 with different amounts of ATBC or PBAT with T_g values of −82 and −33°C, respectively. In the former case, the torque decreased with increasing

TABLE IV
T_g, T_{cc}, T_m, and Enthalpies of the P1/PBAT Blends Containing Different Amounts of ATBC

Sample	T_g (°C)	ΔH_{cc} (J/g)[a]	T_{cc} (°C)	ΔH_m (J/g)[a,b]	T_m (°C)	ΔH_{mc} (J/g)[a,b]	Percentage crystallinity of PLA after quenching[a,c,d]
P1p10	60.1	−2.6	132	2.6	153	0	~ 0
P1p10atbc5	53.4	−17.2	117	18.9	148	1.7	1.8
P1p10atbc10	48.2	−21.3	109	21.6	145	0.2	0.3
P1p10atbc25	25.3	−23.8	83	20.0	144	0	0
P1p20	60.3	−2.9	131	3.9	152	1.1	1.4
P1p20atbc5	55.5	−13.1	123	17.1	151	3.9	5.5
P1p20atbc10	48.1	−18.0	107	21.3	144	3.3	4.9
P1p20atbc25	34.5	−16.7	85	20.5	146	3.7	6.0

[a] The enthalpies and crystallinity were calculated with the actual PLA content.
[b] In the calculation, ΔH_m of the PBAT was neglected.
[c] For the calculation of crystallinity content, the enthalpy of totally crystalline PLA was assumed to be $\Delta H_0 = 93$ J/g.[17]
[d] T, PBAT is the glass transition temperature of the PBAT.

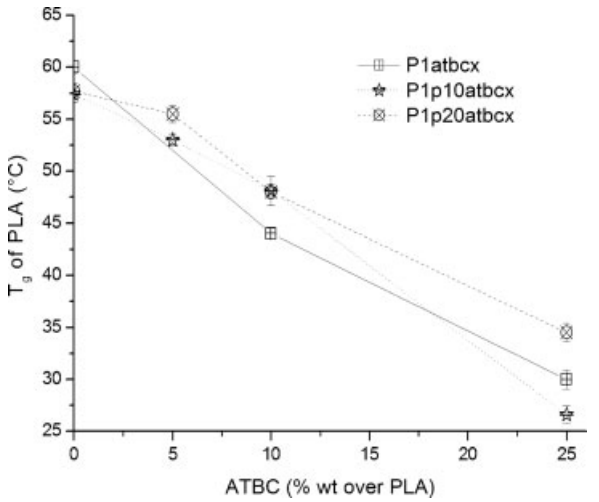

Figure 3 Trend of T_g against the percentage by weight of ATBC over PLA.

amount of additive, whereas in the latter case, a slight increase in the torque was observed. At the same time, the T_g of PLA ($T_{g\mathrm{PLA}}$) decreased with increasing amount of added ATBC, whereas the addition of PBAT did not result in any appreciable change.

The decrease in both torque and T_g in the P1/ATBC mixtures was related to the complete miscibility of ATBC with P1, which was in agreement with the morphological characterization (Fig. 1). The appearance of an inhomogeneous system at 25% ATBC revealed the probable overcoming of the solubility threshold for ATBC in the PLA phase. On the contrary, the addition of PBAT resulted in the well-known phase separation,[29,30] as evidenced by the SEM analysis of the compression-molded films, where the presence of round PBAT domains in the PLA matrix were revealed.

The analysis of the second heating scan in the DSC thermograms (heating rate = 10°C/min) of the P1/ATBC mixtures evidenced cold crystallization peaks whose enthalpy increased with increasing ATBC content (Table II). The positive values of ΔH_{mc}, obtained by the summation of the enthalpy of crystallization occurring during the heating step (ΔH_{cc}) and the melting enthalpy (ΔH_m), revealed that the crystallization of PLA also occurred during the rapid cooling procedure. In comparison with these results in the presence of PBAT, the cold crystallization peaks shifted at higher temperatures, and the involved enthalpy values were lower. In particular, a decrease up to −2.9 J/g with increasing PBAT content was measured. The pure PLA crystallinity developed during the quenching in liquid nitrogen was almost negligible. Similarly, the percentage of PLA crystallinity in the presence of PBAT was almost negligible, and $T_{g\mathrm{PLA}}$ in the blend was quite similar to that of the pure polymer.

The addition of ATBC produced a decrease in the tensile modulus and an increase in the strain at break due to the plasticizer effect.[15] The effect leveled off at 25% addition (Table III), likely because tensile tests were performed at a temperature (27°C) close to the sample glass transition (30.3°C). On the contrary, the addition of PBAT induced a slighter decrease in the tensile modulus, which was in agreement with the development of a multiphase system with PLA as the matrix. Also, a nonnegligible increase in elongation at break (from 13% for crude P1 up to 97% for the P1/PBAT blends) was observed with a content of PBAT of 25 wt % over P1. Hence,

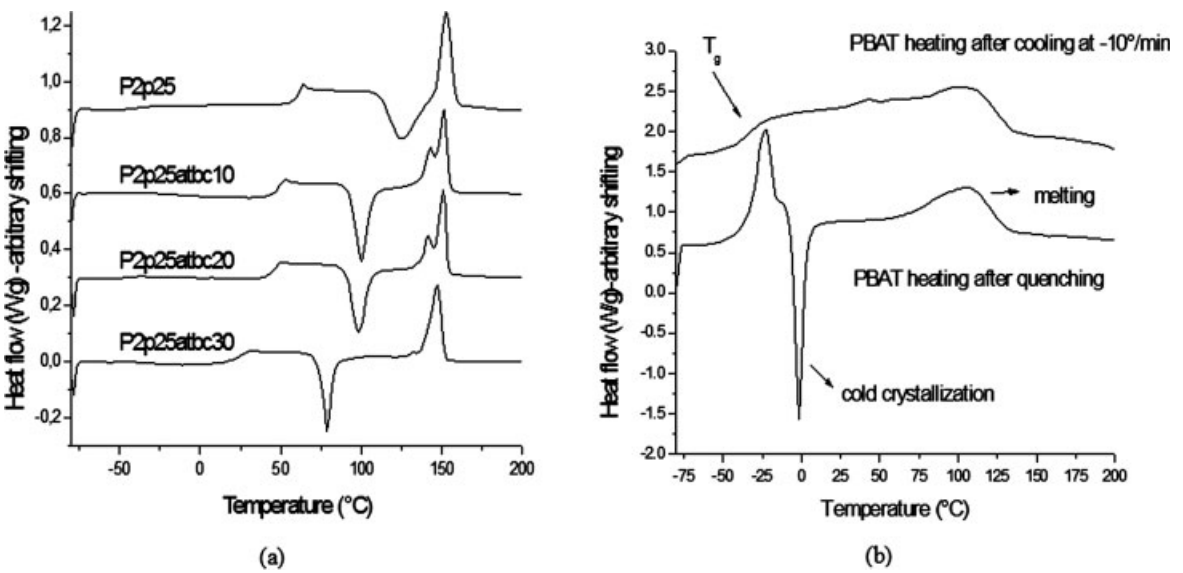

Figure 4 Thermograms recorded for the (a) second heating of P2-based blends and (b) pure PBAT heated after cooling at −10°C/min or quenching in liquid nitrogen.

TABLE V
T_g, T_{cc}, T_m, and Enthalpies of the P2/PBAT Blends Containing Different Amounts of ATBC

Blend	$T_{g\text{PLA}}$ (°C)	$T_{g\text{PBAT}}$ (°C)[d]	T_{cc} (°C)	ΔH_{cc} (J/g)[a]	T_m (°C)	ΔH_m (J/g)[a,b]	ΔH_{mc} (J/g)[a,b]	Percentage crystallinity of PLA after cooling[c]
P2	59.7	—	—	—	—	—	—	
PBAT	—	−33	—	—	104.0	19.4	—	—
P2p25	61.6	−36.7	124.9	−21.3	152.9	21.2	0	0
P2p25atbc10	49.1	−44.0	100.3	−22.8	151.6 143.2	27.3	4.5	4.8
P2p25atbc20	45.7	−49.6	98.3	−22.5	151.2 143.8	26.0	3.5	3.8
P2p25atbc30	23.3	nd	79.2	−21.3	147.5	24.5	3.2	3.4

The values for the pure polymers are also reported. nd = not determined.
[a] The enthalpies and crystallinity were calculated with the actual PLA content.
[b] In the calculation, ΔH_m of the PBAT was neglected.
[c] For the calculation of crystallinity content, the enthalpy of totally crystalline PLA was assumed to be $\Delta H_0 = 93$ J/g.[17]
[d] $T_{g\text{PBAT}}$ is the glass transition temperature of the PBAT.

the PBAT dispersed phase probably allowed the yielding of the matrix when a proper morphology was reached in terms of PBAT domain interparticle distance, which was in agreement with studies about the toughening of thermoplastic polymers.[34,35]

PLA/PBAT/ATBC blend properties

The increase in the ATBC content produced a decrease in the final torque values for all of the examined blends (Fig. 2). In the ternary blends, T_g decreased with increasing ATBC content with a similar trend, already observed in PLA/ATBC compounds, for the P1 and P1/PBAT blends (Table IV). T_g for the ternary blends was higher than that of the P1/ATBC binary blends. The difference was less evident when the content of ATBC was higher, as evidenced in the lowest T_g observed for the 90/10 PLA/PBAT with 25% ATBC (Fig. 3). The melting temperature (T_m) and crystallization temperature (T_{cc}) also decreased with increasing ATBC content, whereas the corresponding enthalpies increased. However, the effect of ATBC addition on the thermal properties was more effective in 90/10 P1/PBAT than in the 80/20 P1/PBAT blends.

The PLA crystallinity developed during quenching was almost negligible in the plasticized P1/PBAT 90/10 system.

The use of P2 instead of P1 did not seem to affect the thermal behavior ($T_{g\text{PLA}}$, T_{cc}, ΔH_{cc}, T_m, and ΔH_m) of the ternary blends [Fig. 4(a)]. In the 75/25 P2/PBAT blend, the T_g values of both polymers slightly increased with respect to those of the pure polymers [Fig. 4(b), Table V]. Also, in the presence of ATBC, the T_g values of both PLA and PBAT (Table V) decreased with increasing ATBC content, which thus confirmed the presence of ATBC in both polymeric amorphous phases. The appearance of a second melting peak of PLA at lower temperatures in the ternary blends [Fig. 4(a)] was in accordance with the results reported in the literature for PPG as plasticizer of PLA[22] and, consequently, could be attributed to the lower stability of crystals undergoing macromolecular reorganization during heating. During the cooling step at −10°C/min, the developed crystallinity was less than 5%, and it was independent of the ATBC content.

The tensile modulus of the plasticized blends [Fig. 5(a)] showed that the ATBC content resulted in effective 80/20 P1/PBAT blend stiffness modulation, as the trend of modulus as a function of ATBC content was found to be almost linear. On the contrary, the 90/10 P1/PBAT blends showed a drastic drop in the modulus between 12 and 18 wt % ATBC over P1, with a trend similar to that of pure P1.[15] The general trend of strain at break was similar in the 80/20 and 90/10 blends for ATBC contents higher than 10% and different for lower percentages of ATBC [Fig. 5(b)]. The strain at break decreased in the 80/20 blends starting from a value of 97%, whereas the corresponding values for the 90/10 blend increased according to the behavior of pure PLA.

By measurement of the values of the dispersed PBAT domain diameter, the interparticle distance (ID) was calculated as follows:[36,37]

$$\mathrm{ID} = d[(\pi/6\phi_r)^{1/3} - 1] \quad (1)$$

where d is the dispersed phase diameter and ϕ_r is the soft-phase volume fraction. A general increase in ID was observed with increasing amount of ATBC [Fig. 5(c)], which was more evident in the 80/20 P1/PBAT blends.

The typical stress–strain curves of P2, P2p25, and P2p25atbc20 are compared in Figure 6. The P2-based 75/25 PLA/PBAT blends showed an effective increase in the strain at break as a function of ATBC

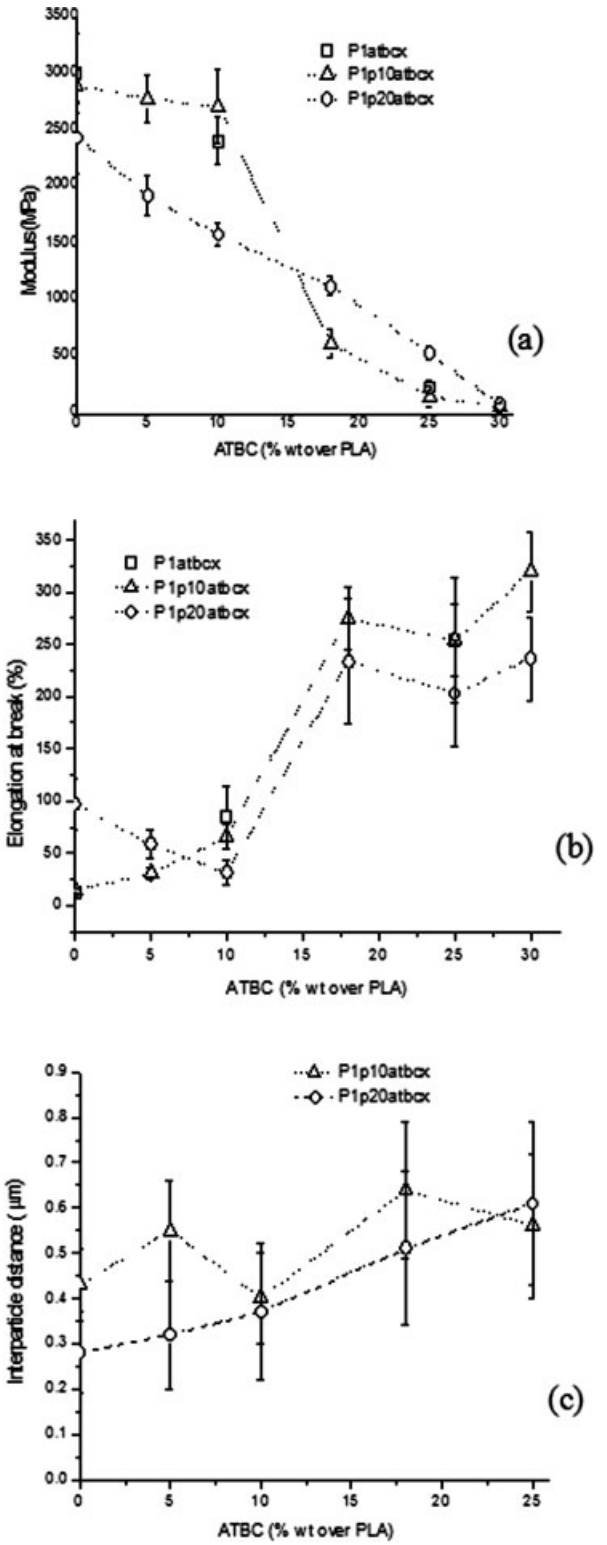

Figure 5 (a) Tensile modulus, (b) elongation at break, and (c) interparticle distance of the compression-molded films of P1 and P1/PBAT as a function of ATBC content.

content in all of the investigated composition range (Table VI).

In good agreement with the diameter calculation, the SEM pictures of the blends showed that the addition of ATBC only slightly modified the dispersed phase diameter in the 90/10 P1/PBAT (Fig. 7, left) and 75/25 P2/PBAT (Fig. 8) blends. On the contrary, it induced an evident increase in the dispersed phase diameter in the 80/20 P1 blends (Fig. 7, right) with increasing ATBC content.

Permeability tests (Table VII) performed on the PLA films showed that the simultaneous addition of PBAT and ATBC caused different permeability increases for different gases (13, 42, and 69% for water vapor, oxygen, and carbon dioxide, respectively), which suggests the possibility of modulation of the permeability by acting on the composition. In addition, the preliminary results on the selectivity seem to indicate that the ternary blends films showed a better selectivity for CO_2 with respect to O_2 and a lower selectivity to water vapor with respect to O_2.

DISCUSSION

To better analyze the plasticization of the binary PLA/PBAT system, the different solubilities of ATBC in the PLA and PBAT phases were considered. In particular, both the PLA and PBAT phases were plasticized by ATBC, as shown by the shift to lower T_g's in both polymers in the P2-based blends (Table VI).

We carried out the evaluation of the concentration of ATBC in the PLA phase by taking into account the $T_{g\mathrm{PLA}}$ trend as a function of ATBC percentage by weight (c_{PLA}) in the pure PLA (Table II). In particular, we carried out a best-fitting mathematical procedure by assuming a first-order exponential decay provided by eq. (2):

$$T_{g\mathrm{PLA}} = 20.7 + 39.4e^{-c_{\mathrm{PLA}}/18.3} \tag{2}$$

Equation (2) allowed the calculation of c_{PLA} in the blends by consideration of the glass-transition values obtained by the DSC analysis. The ATBC percentage by weight in pure PBAT (c_{PBAT}) was calculated on the basis of mass balance considerations. The partition coefficient (the $c_{\mathrm{PBAT}}/c_{\mathrm{PLA}}$ ratio, or K) was further calculated. For comparison, the evaluation of the concentration of ATBC in the PLA phase was also carried out by application of the Fox law [eq. (3)]:

$$\frac{1}{T_{g\mathrm{PLAB}}} = \frac{w_1}{T_{g\mathrm{ATBC}}} + \frac{w_2}{T_{g\mathrm{PLA}}} \tag{3}$$

where $T_{g\mathrm{PLAB}}$, $T_{g\mathrm{ATBC}}$, and $T_{g\mathrm{PLA}}$ are the T_g's of PLA in the blends, pure ATBC, and pure PLA, respectively, and w_1 and w_2 are the volume fractions of ATBC and PLA, respectively, in the PLA phase. The concentration of ATBC into the PBAT phase was

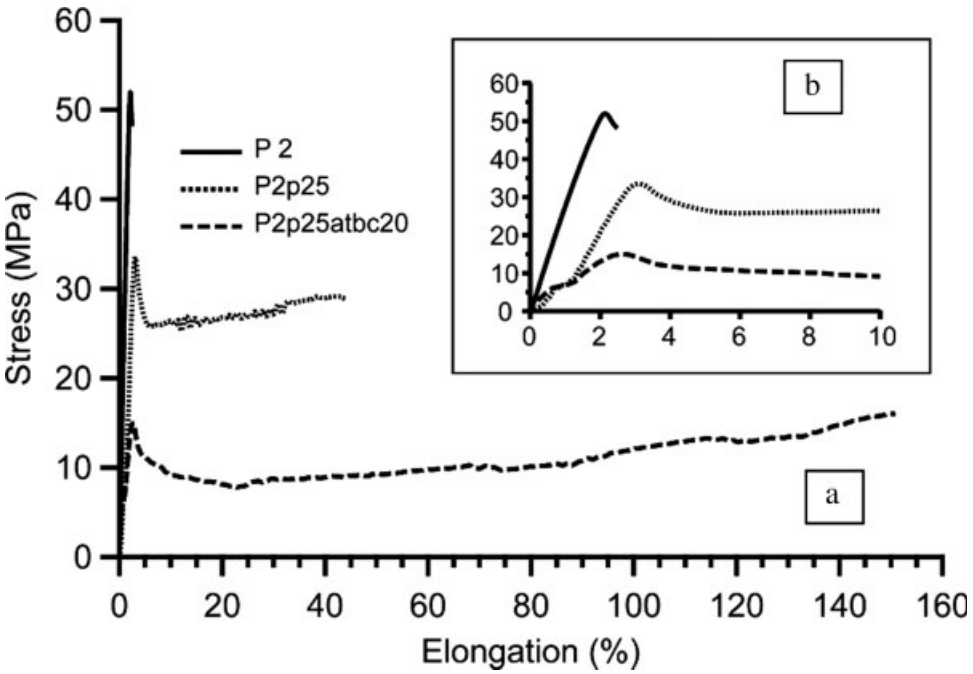

Figure 6 (a) Typical stress–elongation curves of neat P2, P2p25, and P2p25atbc20. (b) Enlargement of the curves for values of elongation lower than 10%.

evaluated by mass balance, which thus allowed the calculation of the concentration ratio calculated with the Fox equation for the determination of the c_{PLA} and c_{PBAT} (K_{Fox}) values. These values were higher than the K values obtained with eq. (2). However, the calculated concentration of ATBC was higher in the PBAT phase (Table VIII) than in the PLA phase despite PBAT being the minor phase. Hence, ATBC was preferentially solubilized by the minor phase. For the highest amount of added ATBC, the values of the partition coefficient K could not be calculated, whereas the values of K_{Fox} were lower than those obtained with lower ATBC contents for the three different blend compositions, which suggested a possible saturation of the minor phase under these conditions. The preferential solubilization in the PBAT phase was attributed to the different local dipole values for the different systems. Indeed, the dipole momentum of ATBC in its minimum energy configuration was estimated to be 4.073 Debye. For a short PLA chain (20 chain atoms), the same estimation gave 3.223 Debye, whereas for a PBAT short chain (26 chain atoms), it gave 4.132 Debye. Therefore, the observed preferential solubilization of ATBC in the PBAT phase was likely due to the closer polarity of the two species.

The preferential solubilization was consistent with the observed increase in T_{gPLA} (Fig. 4) and the reduction in ductility (Fig. 5) in the ternary blends. When a low amount of ATBC was added to the P1/PBAT blends, a different trend of strain at break was observed, which changed from the 90/10 to 80/20 composition [Fig. 5(b)]. This result could be rationalized on the basis of a different phase morphology development. In fact, the 90/10 blends showed a phase morphology that was only slightly influenced by the addition of ATBC. The tensile behavior of the 80/20 blend was different, as the addition of 20% of

TABLE VI
Tensile Properties, Dispersed Phase Diameter, and Interparticle Distance of the P2/PBAT 75/25 Blends Plasticized with ATBC

Sample	Modulus (MPa)	At yield		At break		Diameter (μm)	Interparticle distance (μm)
		Stress (MPa)	Strain (%)	Stress (MPa)	Strain (%)		
P2	2893 ± 235	48 ± 5	2.6 ± 0.2	37 ± 5	8 ± 4	—	—
P2p25	1935 ± 110	38 ± 2	3.0 ± 0.2	31 ± 3	47 ± 25	1.2 ± 0.5	0.3 ± 0.1
P2p25atbc10	1778 ± 111	18 ± 2	1.7 ± 0.1	18 ± 2	87 ± 32	1.5 ± 1.0	0.4 ± 0.3
P2p25atbc20	870 ± 70	15 ± 2	2.9 ± 0.3	18 ± 4	150 ± 38	1.4 ± 1.0	0.4 ± 0.3
P2p25atbc30	62 ± 29	—	—	18 ± 5	250 ± 60	1.8 ± 0.9	0.5 ± 0.2

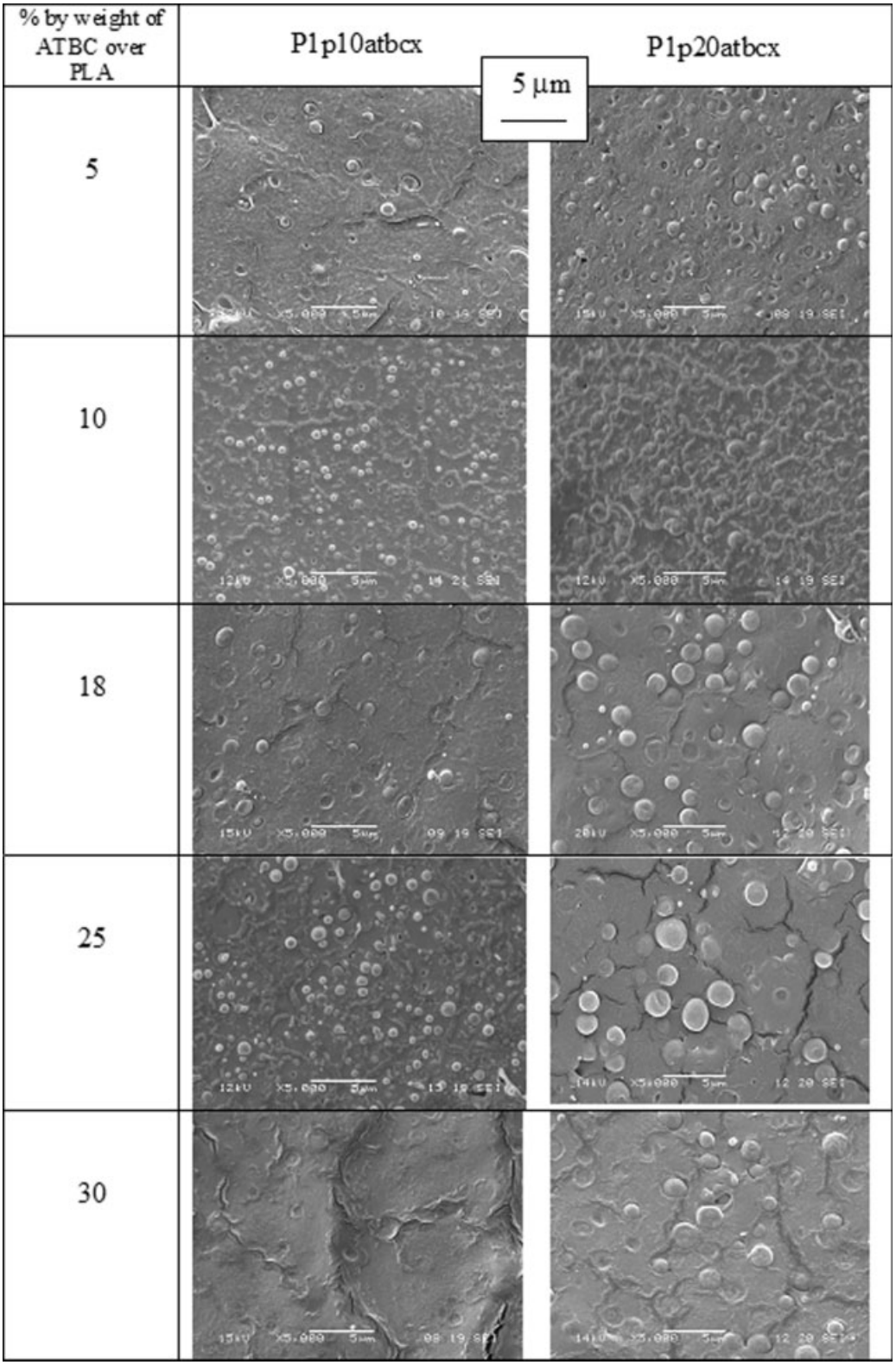

Figure 7 SEM micrographs of the cryogenic fractures of the compression-molded films made of 90/10 and 80/20 wt/wt P1/PBAT blends obtained by the addition of different amounts of ATBC.

PBAT to pure PLA resulted in an improvement in the elongation at break (from 13 to 98%). In fact, in this case, a proper value for the interparticle distance was achieved [Fig. 5(c)], which allowed the change of failure mode from brittle to ductile, as reported by Jiang et al.[37] The addition of ATBC resulted in the increase in the PBAT dispersed phase diameter (Fig. 6).

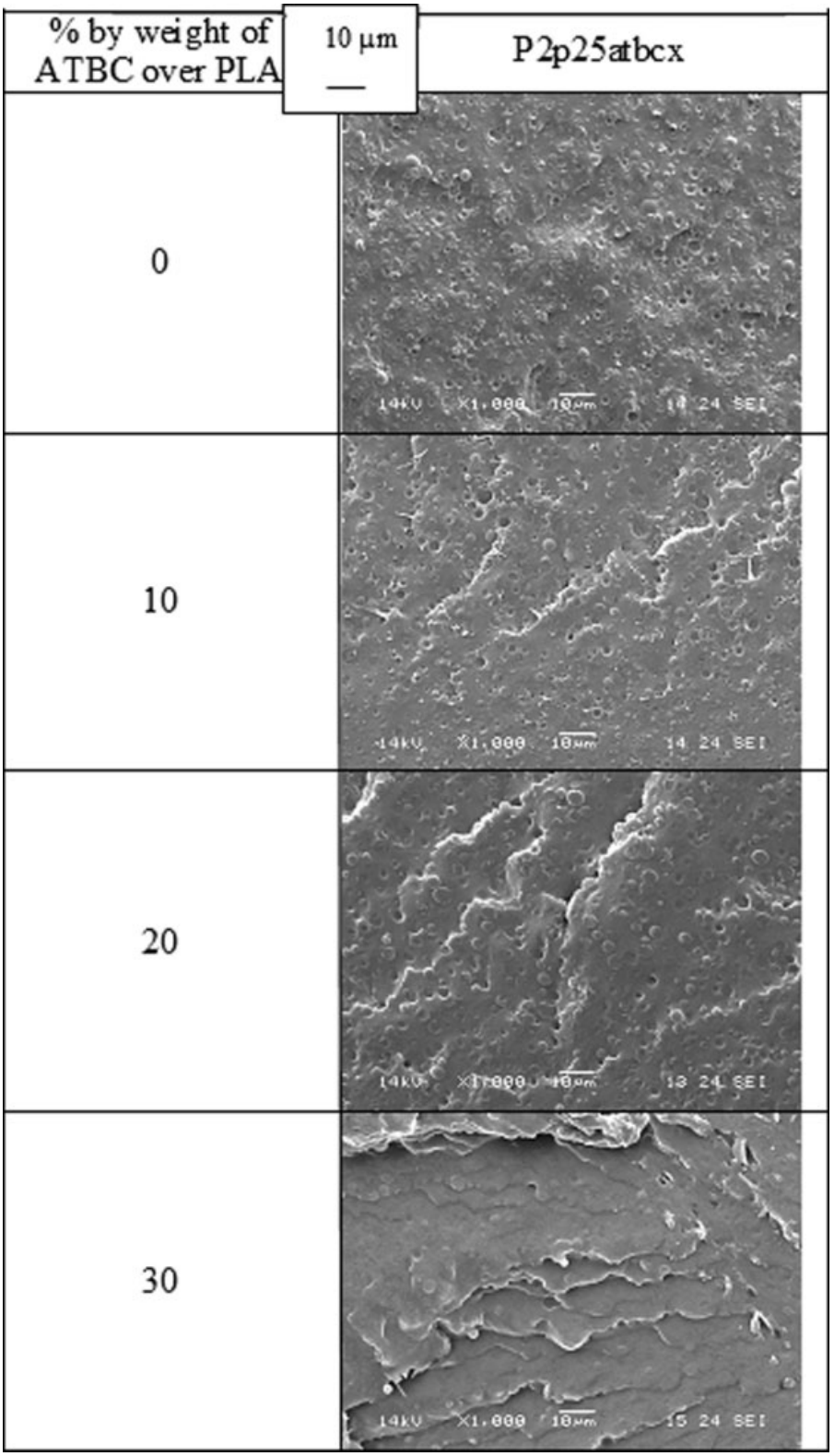

Figure 8 SEM micrographs of the cryogenic fractures of the compression-molded films made of 75/25 wt/wt P2/PBAT blends obtained by the addition of different amounts of ATBC.

In fact, the addition of ATBC reduced the viscosity ratio between the matrix and dispersed phase because of the preferential solubilization of ATBC in PBAT, which resulted in an increase in the dispersed domain diameter.[34] Moreover, the general reduction in viscosity favored the coalescence of the dispersed

TABLE VII
Permeability Tests Performed on the P1-Based Films

Sample	O_2Tr[a] (cc/m^2 24 h)	WVTr[a] (g m^{-2} 24 h^{-1})	CO_2Tr[a] (cc m^{-2} 24 h^{-1})	CO_2Tr/O_2Tr	$WVTr/O_2Tr$
P1	177	80	797	4.5	0.45
P1PBAT10	nd	70	nd	nd	nd
P1atbc10	nd	97.8	nd	nd	nd
P1p10atbc10	253	90.7	1348	5.3	0.36

[a] O_2Tr is the transmission rate of O_2; WVTr is the transmission rate of water vapor; CO_2Tr is the transmission rate of CO_2. nd, not determined.

domains, which adversed the toughening mechanism. A different trend was observed for the P2/PBAT blends, where a decrease in the elongation at break was not observed when ATBC was added. The difference between the two systems was ascribed to the higher viscosity of P2, which limited the coalescence phenomena. Moreover, the different composition could play an important role. In fact, a higher amount of soft phase (25%) granted the conservation of the proper conditions of interparticle distance necessary to achieve the toughening.[35,38] In particular, the blends showed an interparticle distance in the limited range 0.3–0.5 μm. Hence, the toughening mechanism was not perturbed by the addition of ATBC in this latter case.

CONCLUSIONS

In this study, the addition to PLA of a low-molecular-weight plasticizer (ATBC) and a biodegradable polyester (PBAT) was investigated as strategies for improving the flexibility of the material. Both additives resulted in improved ductility when they were added to pure PLA, with the former behaving as a plasticizer and lowering the glass transition up to 27°C and the latter behaving as an immiscible toughening agent.

TABLE VIII
Concentration of ATBC in the PLA and PBAT Phases and the c_{PBAT}/c_{PLA} (K) Constants

$\%w_{ATBC}$[a]	c_{PLA}[b]	c_{PBAT}[b]	s_c[c]	K	K_{Fox}
P1p10atbc$x$					
5	0.034	0.141	0.004	4.1	6.2
10	0.066	0.306	0.006	4.6	8.6
25	0.394	—	0.015	—	4.9
P1p20atbc$x$					
5	0.023	0.108	0.004	4.7	6.5
10	0.067	0.133	0.004	2.0	3.8
25	0.192	0.230	0.007	1.2	4.8
P2p25atbc$x$					
10	0.060	0.119	0.002	2.0	3.4
20	0.083	0.349	0.006	4.2	6.7
30	0.498	—	0.0228	—	3.4

[a] Weight percentage with respect to PLA.
[b] The concentrations are expressed as weight fractions of ATBC in the PLA or PBAT phase.
[c] We calculated the standard deviation related to the concentration (s_c) by considering that $s_c = s_{Tg}[723.13/(T_{gPLA})^2]^{0.5}$ on the basis of eq. (2). g_{Tg} is the standard deviation of T_{gPLA}

The addition of ATBC to the PLA/PBAT blends allowed the plasticization of the material, which resulted in a strain at break higher than 150% when about the 20% ATBC with respect to PLA was added. The plasticization was effective for different compositions (90/10, 80/20, and 75/25 PLA/PBAT) and for two different PLAs (P1 and P2).

The preferential solubilization of ATBC in the PBAT phase was revealed by the analysis of the thermal properties of the blends, and it was attributed to the similar local dipole values of ATBC and PBAT. Thus, the PBAT domains in the PLA matrix system behaved as reserves of ATBC and reduced the kinetic of migration to the film surface[13] of the low-molecular-weight plasticizer with a resulting positive effect on the stability of the mechanical properties over time also under different conditions of use.

The addition of at least 20% PBAT to PLA resulted in the toughening of the fragile PLA matrix, but plasticization with a low amount of ATBC resulted in an improvement in the elongation at break only in proper conditions. In particular, the addition of the plasticizer reduced the toughening effect because of the increase in the interparticle distance between the PBAT domains. However, this effect was less evident in the 75/25 P2/PBAT blends. Hence, control of phase morphology development was achieved by proper selection of the PLA and the composition of the PLA/PBAT blend.

The authors thank ExtraSolution and Dr. Flavia Imma Di Cuia for help with the permeability tests, and Dr. Eng.

Consuelo Escrig Rondan of Instituto Tecnologico del Plastico (AIMPLAS) (Spain) is also thanked for helpful discussion.

References

1. Vink, E. T. H.; Rabago, K. R.; Glassner, D. A.; Gruber, P. R. Polym Degrad Stab 2003, 80, 403.
2. Kamm, B.; Kamm, M.; Gruber, P. R.; Kromus, S. In Biorefineries—Industrial Processes and Products: Status Quo and Future Directions; Kamm, B.; Gruber, P. R.; Kamm, M., Eds.; Wiley-VCH: Weinheim, 2006; p 1.
3. Dornburg, V.; Faaij, A.; Patel, M.; Turkenburg, W. C. Res Conser Recycling 2006, 46, 377.
4. Auras, R.; Harte, B.; Selke, S. Macromol Biosci 2004, 4, 835.
5. Auras, R. A.; Singh, S. P.; Singh, J. J. Packag Technol Sci 2005, 18, 207.
6. Plackett, D. V.; Holm, V. K.; Johansen, P.; Ndoni, S.; Nielsen, P. V.; Sipilainen-Malm, T.; Södergard, A.; Verstichel, S. Packag Technol Sci 2006, 19, 1.
7. Rahman, M.; Brazel, C. S. T. Prog Polym Sci 2004, 29, 1223.
8. Martin, O.; Averous, L. Polymer 2001, 42, 6209.
9. Shibata, M.; Someya, Y.; Orohara, M.; Miyoshi, M. J Appl Polym Sci 2006, 99, 2594.
10. Ljungberg, N.; Andersson, T.; Wesslen, B. J Appl Polym Sci 2003, 88, 3239.
11. Pillin, I.; Montrelay, N.; Grohens, Y. Polymer 2006, 47, 4676.
12. Zhang, J. F.; Sun, X. Macromol Biosci 2004, 4, 1053.
13. Labrecque, L. V.; Kumar, R. A.; Davé, V.; Gross, R. A.; McCarthy, S. P. J Appl Polym Sci 1997, 66, 1507.
14. Kranz, H.; Ubrich, N.; Maincent, P.; Bodmeier, R. J Pharm Sci 2000, 89, 1558.
15. Baiardo, M.; Frisoni, G.; Scandola, M.; Rimelen, M.; Lips, D.; Ruffieux, K.; Wintermantel, E. J Appl Polym Sci 2003, 90, 1731.
16. Ljungberg, N.; Wesslen, B. Polymer 2003, 44, 7679.
17. Ljungberg, N.; Wesslen, B. Biomacromolecules 2005, 6, 1789.
18. Sheth, M.; Ananda Kumar, R.; Davé, V.; Gross, R. A.; McCarthy, S. P. J Appl Polym Sci 1997, 66, 1495.
19. Pluta, M.; Paul, M. A.; Alexandre, M.; Dubois, P. J Polym Sci Part B: Polym Phys 2006, 44, 312.
20. Kulinski, Z.; Piorkowska, E. Polymer 2005, 46, 10290.
21. Piorkowska, E.; Kulinski, Z.; Galeski, A.; Masirek, R. Polymer 2006, 47, 7178.
22. Kulinski, Z.; Piorkowska, E.; Gadzinowska, K.; Stasiak, M. Biomacromolecules 2006, 7, 2128.
23. Ljungberg, N.; Colombini, D.; Wesslen, B. J Appl Polym Sci 2005, 96, 992.
24. Passerini, N.; Craig, D. Q. M. J Controlled Release 2001, 73, 111.
25. Furukawa, T.; Sato, H.; Murakami, R.; Zhang, J.; Duan, Y. X.; Noda, I.; Ochiai, S.; Ozaki, Y. Macromolecules 2005, 38, 6445.
26. Shibata, M.; Inoue, Y.; Miyoshi, M. Polymer 2006, 47, 3557.
27. Tsuji, H.; Ishizaka, T. Int J Biol Macromol 2001, 29, 83.
28. Na, Y. H.; He, Y.; Shuai, X.; Kikkawa, Y.; Doi, Y.; Inoue, Y. Biomacromolecules 2002, 3, 1179.
29. Yang, J. M.; Chen, H. L.; Yu, J. W.; Hwang, J. C. Polym J 1997, 29, 657.
30. Liu, T. Y.; Lin, W. C.; Yang, M. C.; Chen, S. Y. Polymer 2005, 46, 12586.
31. Jiang, L.; Wolcott, M. P.; Zhang, J. Biomacromolecules 2006, 7, 199.
32. Shibata, M.; Teramoto, N.; Inoue, Y. Polymer 2007, 48, 2768.
33. Pluta, M.; Paul, M. A.; Alexandre, M.; Dubois, P. J Polym Sci Part B: Polym Phys 2006, 44, 299.
34. Harrats, C.; Groeninckx, G. In Modification and Blending of Synthetic and Natural Macromolecules; Ciardelli, F.; Penczek, S., Eds.; Kluwer Academic: Dordrecht, 2004; p 155.
35. Akkapeddi, K. In Reactive Polymer Blending; Baker, W. E.; Scott, C. E.; Hu, G. H., Eds.; Hanser: Munich, 2001; p 207.
36. Wu, S. Polymer 1985, 26, 1855.
37. Jiang, W.; Liang, H.; Liang, B. Polymer 1998, 39, 4437.
38. Galeski, A. Prog Polym Sci 2003, 28, 1643.